

Classical resonance interactions and Josephson junction in macroscopic quantum dynamics

V.N. Pilipchuk

Wayne State University, Detroit, MI

e-mail: pilipchuk@wayne.edu

March 30, 2022

Abstract

It is shown that the classical dynamics of 1:1 resonance interaction between two identical linearly coupled Duffing oscillators is equivalent to the symmetric (non-biased) case of ‘macroscopic’ quantum dynamics of two weakly coupled Bose-Einstein condensates. The analogy develops through the boson Josephson junction equations, however, reduced to a single conservative energy partition (EP) oscillator. The derived oscillator is solvable in quadratures, furthermore it admits asymptotic solution in terms of elementary functions after transition to the action-angle variables. Energy partition and coherency indexes are introduced to provide a complete characterization of the system dynamic states through the state variables of the EP oscillator. In particular, nonlinear normal and local mode dynamics of the original system associate with equilibrium points of such oscillator. Additional equilibrium points - the local modes - may occur on high energy level as a result of the symmetry breaking bifurcation, which is equivalent to the macroscopic quantum self-trapping effect in *boson* Josephson junction. Finally, since the Hamiltonian of EP oscillator is always quadratic with respect its linear momentum, the idea of second quantization can be explored without usual transition to the rigid pendulum approximation.

1 INTRODUCTION

The present study brings attention to the analogy between 1:1 resonance dynamics of coupled classical Duffing oscillators and macroscopic quantum dynamics of coupled Bose-Einstein condensates [2]. Despite of quite different physical contents the resultant equations for both types of interaction appear to have surprisingly the same form of boson Josephson junction (BJJ) tunneling equations [27] [25]. These represent a classical single degree-of-freedom Hamiltonian system whose conjugate states are the fractional population disbalance and phase difference. In macroscopic quantum dynamics, such equations are

eventually obtained from the nonlinear Schrödinger (Gross-Pitaevskii) equation [5] [23] by representing the corresponding wave function as a superposition of two wave functions [27] [25]. In the case of classical resonance dynamics, the BJJ equations are obtained after specific coordinate transformation by applying parameter variation and conventional averaging techniques to the differential equations of motion of interacting oscillators. Further analogies are revealed by establishing the links between qualitative features of the BJJ equations and the corresponding physical effects developed in both classical and macroscopic quantum dynamics. In particular, specifics of the energy exchange between nonlinear oscillators due to their 1:1 resonance and so-called nonlinear normal mode motions are discussed first. It is known that, during the normal mode motions [26] [30], the energy partition between the oscillators from one cycle to another is fixed so that there is no energy flow between the oscillators. However, when the initial states of oscillators are out of compliance with any of the normal modes, the oscillators slowly exchange by some portion or even all of the energy in a beat-wise manner. Such beating phenomena have been in focus of nonlinear physics and physical mechanics for few decades by very different theoretical and practical reasons [8] [6]. Usually, the beat dynamics are described through the transition to amplitude-angle or similar coordinates followed by averaging the new equations over one cycle of vibration. The resultant system may appear to have one or may be several integrals dictated by the system's symmetry [6]. These types of integrals actually provide the description for the energy exchange between the interacting oscillators. Recently, based on the detailed parametric study of phase trajectories, the notion of limiting phase trajectory was introduced [13] [14] [12]. It was noticed that, in the limit when the entire energy of the system swings from one oscillator to another, the descriptive phase angles resemble state variables of impact oscillators with non-smooth temporal shapes. The importance of this observation is that it provides asymptotic simplifications for the cases extremely opposite to the normal modes. Further, analytical algorithms of nonsmooth temporal transformations [20] [21] were adapted to build approximate analytical solutions for limiting phase trajectories [17] [16] [29]. In the present work, it is shown that the phase variable, which determines the energy partition (EP) between the two oscillators, is given by a strongly nonlinear conservative oscillator, which is exactly solvable for any intensity of the energy exchange. Furthermore, the EP oscillator admits two different asymptotic limits associated with the vanishing or maximal possible intensities of beats in which the oscillator becomes harmonic or vibro-impact, respectively. In particular, the impact limit corresponds to the limiting phase trajectory on which the energy exchange involves the total energy of the system. Finally, it is shown that first integral of the EP oscillator completely determines necessary and sufficient conditions for the nonlinear mode localization phenomenon [26] [30]. It is shown that vibrations near nonlinear local modes of coupled oscillators are equivalent to the macroscopic quantum self-trapping (MQST) effect. As discussed earlier [25], there are two types of MQST, such as running-phase MQST and π -phase MQST. Note that the BJJ captures both types of MQST whereas the superconductor Josephson junction (SJJ) rigid pendulum approximation ignores the

π -phase MQST. An early overview and introduction to SJJ can be found in [1]. According to this theory, a single wave function associates with a macroscopic number of electrons which are assumed to condense in the same quantum (superconductive) state. When two superconductors are close enough to each other, practically at about 30 Å, the superconductors begin to interact through the tunneling effect such that at about 10 Å between the superconductors their macroscopic quantum phases cannot be viewed as independent any more and must be described as a single system [1]. In a similar way, it is impossible to separately consider two even weakly coupled classical oscillators when they resonate. This is due to the fact that slowly oscillating resonance energy flows between the oscillators cannot be ignored anymore and must be interpreted as a new system. As mentioned above, such new system represents a strongly nonlinear conservative oscillator with quite interesting physical and mathematical properties. Surprisingly enough, the basic case of such oscillator has been known for several decades as unique example of strongly nonlinear exactly solvable oscillator with no relation to any physically meaningful situation [7], except few phenomenological applications [19] [3] [22]. Sections 2 through 5 describe the methodology based on the classical model of coupled Duffing oscillators. In Section 6 it is shown that the resultant 1:1 classic resonance equations take the form of BJJ equations. Then, the BJJ derivation in macroscopic quantum dynamics is briefly recalled for comparison. Finally, the analogies and physical meaning of the BJJ variables in classical and quantum dynamical cases are discussed.

2 NONLINEAR BEATS

2.1 Coupled nonlinear oscillators

Let us consider a system of two identical linearly coupled unit-mass oscillators (Fig.1) described by Hamiltonian

$$H = \frac{1}{2} (v_1^2 + v_2^2) + \Pi(u_1) + \Pi(u_2) + \frac{1}{2}b(u_1 - u_2)^2 \quad (1)$$

where u_i and v_i ($i = 1, 2$) are the coordinates and linear momenta, respectively, $\Pi(u_i)$ is an even analytic function describing the potential energy for each of the two oscillators, and b is the coupling stiffness, which is assumed to be relatively weak, $b/\Pi''(0) \ll 1$.

Introducing the parameters, $\Omega = \sqrt{\Pi''(0) + b}$ and $\varepsilon = b\Omega^{-2}$, and subtracting the parabolic component from the potential energy,

$$\Pi(u) - \frac{1}{2}\Pi''(0)u^2 \equiv \varepsilon U(u) \quad (2)$$

brings Hamiltonian (1) to the form, which incorporates the additional assumption that both nonlinearity and coupling are of the same order of magnitude, ε ,

$$H = \frac{1}{2} (v_1^2 + v_2^2) + \frac{1}{2}\Omega^2 (u_1^2 + u_2^2) + \varepsilon [U(u_1) - \Omega^2 u_1 u_2 + U(u_2)] \quad (3)$$

Note also that the coupling is represented now in somewhat canonical form after the non-coupled terms of the interaction energy (1), $bu_i^2/2$, have been associated with the corresponding oscillators. The differential equations of motion are given by

$$\dot{u}_i = \frac{\partial H}{\partial v_i}, \quad \dot{v}_i = -\frac{\partial H}{\partial u_i} \quad (4)$$

or

$$\begin{aligned} \dot{u}_1 &= v_1 \\ \dot{u}_2 &= v_2 \\ \dot{v}_1 &= -\Omega^2 u_1 + \varepsilon[\Omega^2 u_2 - U'(u_1)] \\ \dot{v}_2 &= -\Omega^2 u_2 + \varepsilon[\Omega^2 u_1 - U'(u_2)] \end{aligned} \quad (5)$$

As $\varepsilon \rightarrow 0$, system (5) degenerates into two identical harmonic oscillators whose total energies are separately conserved. At non-zero ε , the oscillators become non-linear and coupled with each other in such way that one of the oscillators is loaded proportionally to the displacement of another oscillator. Since system (5) is perfectly symmetric and conservative, it is reasonable to assume a relatively slow energy exchange between the oscillators due to the weak coupling. In order to describe the energy exchange dynamics in physically meaningful terms, let us introduce a new set of variables as follows $\{u_1, v_1, u_2, v_2\} \rightarrow \{K(t), \theta(t), \delta(t), \Delta(t)\}$:

$$\begin{aligned} u_1 &= \sqrt{K} \cos\left(\frac{\theta}{2} + \frac{\pi}{4}\right) \cos \delta \\ v_1 &= -\sqrt{K}\Omega \cos\left(\frac{\theta}{2} + \frac{\pi}{4}\right) \sin \delta \\ u_2 &= -\sqrt{K} \sin\left(\frac{\theta}{2} + \frac{\pi}{4}\right) \cos(\delta + \Delta) \\ v_2 &= \sqrt{K}\Omega \sin\left(\frac{\theta}{2} + \frac{\pi}{4}\right) \sin(\delta + \Delta) \end{aligned} \quad (6)$$

If K , θ , and Δ are constant, and $\delta = \Omega t$, expressions (6) represent the exact general solution of the decoupled set of harmonic oscillators (5), $\varepsilon = 0$. Therefore, relationships (6) implement the idea of parameter variations compensating the perturbation, when $\varepsilon \neq 0$. In order to track the oscillator energies during the vibration process, let us introduce quantities

$$\begin{aligned} E_1 &= \frac{1}{2}(v_1^2 + \Omega^2 u_1^2) = \frac{1}{2}E_0(1 - \sin \theta) \\ E_2 &= \frac{1}{2}(v_2^2 + \Omega^2 u_2^2) = \frac{1}{2}E_0(1 + \sin \theta) \\ E_{12} &= \frac{1}{2}(v_1 v_2 + \Omega^2 u_1 u_2) = -\sqrt{E_1 E_2} \cos \Delta \end{aligned} \quad (7)$$

where

$$E_0 = E_1 + E_2 = \frac{1}{2}\Omega^2 K \quad (8)$$

Expressions (7) and (8) clarify physical meaning of the variables K , θ and Δ participating in transformation (6), while the variable δ is the fast phase associated with the principal temporal rate of the vibrating oscillators. In particular, the quantity K is proportional to the total energy of the decoupled and linearized oscillators, the phase θ characterizes the energy partition between the oscillators, and Δ relates to the phase shift between the oscillators as discussed below. In case $\varepsilon \neq 0$, the energy parameter K has small temporal fluctuations due to the coupling and nonlinear terms in (5). Nevertheless, expressions (7) and (8) can still be used for characterization of the energy distribution between the oscillators. For that purpose, as follows from (7), the interval $-\pi/2 \leq \theta \leq \pi/2$, on which $E_0 \geq E_1 \geq 0$ and $0 \leq E_2 \leq E_0$, is sufficient. In particular, the case $\theta = 0$ corresponds to equipartition, $E_1 = E_2$, under which the system oscillate either out-of-phase ($\Delta = 0$) or in-phase ($\Delta = \pi$) according to the sign convention in (6). It is convenient to deal with one full period of the phase shift Δ within the range $-\pi/2 \leq \Delta \leq 3\pi/2$, including both in-phase and out-of-phase modes.

2.2 Energy partition and coherency indexes

As an alternative to the angular quantities θ and Δ , let us introduce the *energy partition index* P and *coherency index* Q describing the system' vibrating states as follows

$$P = \frac{E_1 - E_2}{E_1 + E_2} = -\sin \theta, \quad -1 \leq P \leq 1 \quad (9)$$

$$Q = \frac{E_{12}}{\sqrt{E_1 E_2}} = -\cos \Delta, \quad -1 \leq Q \leq 1 \quad (10)$$

According to definition (9), the number $P = 0$ indicates the energy equipartition, $E_1 = E_2$, whereas $P = 1$ or $P = -1$ correspond to the case when all the energy belongs to either first or second oscillator, respectively. According to definition (10), the boundaries $Q = 1$ and $Q = -1$ correspond to in-phase and out-of-phase modes, respectively, as illustrated by Figs. 1 and 2.

The derivation of equations for the descriptive phase variables includes substitution of the coordinate transformation (6) in (5), which is in fact the variation of constants procedure, and then implementing the averaging with respect to the fast phase δ as described in Appendix. Assuming the monomial form, $U(u_i) = \alpha u_i^4/4$, such averaging gives

$$\begin{aligned} \dot{K} &= 0 \\ \dot{\theta} &= \varepsilon \Omega \sin \Delta \\ \dot{\Delta} &= -\varepsilon \Omega (\cos \Delta \tan \theta - \kappa \sin \theta) \\ \dot{\delta} &= \Omega + \frac{1}{2} \varepsilon \Omega \left[\cos \Delta \tan \left(\frac{\theta}{2} + \frac{\pi}{4} \right) + \kappa (1 - \sin \theta) \right] \end{aligned} \quad (11)$$

where the following nonlinearity parameter is introduced

$$\kappa = \frac{3\alpha K}{8\Omega^2} \quad (12)$$

The first equation in (11) shows that the energy parameter K remains averagely constant regardless the perturbation parameter ε . The fact that K is constant justifies the use of quantities (7) and (8) for characterization of the energy exchange between the oscillators since neither the coupling nor nonlinear stiffness in (5) can accumulate the energy during one vibration cycle. In order to clarify physical meaning of the parameter κ , consider a single oscillator, $\ddot{u} + \Omega^2 u + \alpha u^3 = 0$, whose mean (over the period) potential energy components, corresponding to linear and nonlinear stiffness terms, are $E_\Omega = \Omega^2 \langle u^2 \rangle / 2$ and $E_\alpha = \alpha \langle u^4 \rangle / 4$, respectively. Assuming the harmonic temporal mode for the coordinate $u(t)$, and taking into account (8) and (12), gives

$$\kappa = \frac{E_\alpha}{E_\Omega} \quad (13)$$

Therefore, κ characterizes the strength of nonlinearity in terms of its relative energy capacity during one vibration cycle. Taking into account (11) and (12), gives also $\dot{\kappa} = 0$. As follows from (11), further complete description of the dynamics can be conducted now in terms of the two phase shift parameters, $\Delta(t)$ and $\theta(t)$; the fast phase $\delta(t)$ is obtained then by integration from the last equation in (11).

As discussed above, the corresponding dynamical system on the phase plane $\Delta - \theta$ will be considered on the rectangular

$$D = \{-\pi/2 \leq \Delta \leq 3\pi/2, -\pi/2 \leq \theta \leq \pi/2\} \quad (14)$$

In the low nonlinearity range, $0 \leq \kappa < 1$, there are two stationary points, $(0, 0)$ and $(\pi, 0)$, corresponding to the out-of-phase and in-phase vibration modes, respectively. However, two more stationary points $(\pm \arccos \kappa^{-1}, 0)$ emerge from zero when the nonlinearity becomes sufficiently strong, $1 \leq \kappa$; see Fig. 1. Geometrical interpretation of the bifurcation at $\kappa = 1$ will be given below in Section 6.1.

3 EP OSCILLATOR

It can be shown by inspection that system (11) admits the integral as follows

$$G \equiv -\cos \Delta \cos \theta + \frac{1}{2} \kappa \cos^2 \theta = \text{const.} \quad (15)$$

Taking into account (15) and eliminating the phase Δ from the second and third equations of system (11), gives a single strongly nonlinear conservative oscillator with respect to the coordinate θ in the form [22], [21]

$$\ddot{\theta} + (\varepsilon\Omega)^2 \left(G^2 \frac{\tan \theta}{\cos^2 \theta} - \frac{1}{8} \kappa^2 \sin 2\theta \right) = 0 \quad (16)$$

Note that the quantity G in equation (16) remains constant only on a fixed dynamic trajectory in the plane θ - Δ but may vary from one trajectory to another. Therefore, the number G (15) must be calculated first by fixing some

point $\{\theta_0, \Delta_0\}$ on the trajectory. Then equation (16) can be solved by making sure that the initial condition $\{\theta(0), \dot{\theta}(0)\}$ corresponds to the fixed trajectory according to the second equation in (11). The parameter κ however can be chosen regardless the dynamics in the plane θ - Δ . According to (7), equation (16) constitutes a principal equation describing the energy exchange between oscillators (5). Moreover, if the function $\theta(t)$ is known, then other two phase variables, Δ and δ , are obtained from system (11) by differentiation and integration.

It is shown therefore that the entire system (11) is exactly solvable in quadratures since general solution of equation (16) can be obtained from its ‘energy’ integral $H_\theta = \text{const}$,

$$H_\theta \equiv \frac{1}{2}\dot{\theta}^2 + (\varepsilon\Omega)^2 \left(\frac{1}{2}G^2 \tan^2 \theta + \frac{1}{16}\kappa^2 \cos 2\theta \right) \quad (17)$$

The dynamics of oscillator (16) essentially depends on the shape of its potential energy within the interval $-\pi/2 < \theta < \pi/2$. In particular, if the parameter κ is small enough, then oscillator (17) has one stable equilibrium position at $\theta = 0$. However, high energy levels of the original system (1), that is large κ , can make the equilibrium position $\theta = 0$ unstable by generating two new (stable) equilibrium positions. Such kind of bifurcation obviously relates to that described at the end of Section 2. According to definition (9), every equilibrium of the oscillator (16) corresponds to a fixed (no beats) energy partition between the oscillators in the original system, in other words, - nonlinear normal mode. Recall that oscillator (16) is obtained after the procedure of averaging has been applied to the original model (5). For validation purposes, Fig. 3 illustrates the behavior of energy partition index (9) based on numerical solutions of both types of models the original model (5) and oscillator (16). The initial configurations are chosen to cover the areas of normal and local modes as illustrated by the model trajectories on configuration planes in Fig. 4. Overall, Figs. 4 through 7 illustrate the dynamic trajectories on configuration planes and the corresponding behaviors of energy partition (9) and coherency (10) indexes, when increasing the energy (nonlinearity) level above the critical point $\kappa = \kappa^* = 1$. Such diagrams give quite complete characterization of the dynamics by showing how the energy is distributed between the oscillators and what is the phase shift between the oscillators at any given time. Note that the derived oscillator (16) captures both local dynamics near separate nonlinear normal modes and drifts over multiple modes, including stable and unstable ones. This essentially complements the theory of nonlinear normal modes in classical dynamics covering mainly periodic normal mode motions and their small neighborhoods [30].

4 ASYMPTOTICS OF BEATS

4.1 Linearized case

When the original system is linear ($\alpha = 0 \implies \kappa = 0$), equation (16) admits explicit analytical solution within the class of elementary functions

$$\theta(t) = \arcsin[\sin \theta_0 \sin \phi(t)] \quad (18)$$

where θ_0 is the amplitude of θ , whereas another constant can be introduced into the phase $\phi(t) = \varepsilon \sec \theta_0 |G| \Omega t$ as an arbitrary temporal shift admitted by equation (16). As mentioned in Introduction, such type of explicit solution has been known for quite a long time with no relation to any physical system [7], however it was used recently in some physical and mechanical applications [19], [3] in a phenomenological way. Although solution (18) holds only for the linear model, $\kappa = 0$, it nevertheless helps to clarify specifics of the behavior of phase variables in nonlinear cases. In particular, substituting (18) in the second equation of (11), gives

$$\Delta(t) = \arcsin \left[\frac{|G| \tan \theta_0 \cos \phi(t)}{\sqrt{1 - \sin^2 \theta_0 \sin^2 \phi(t)}} \right] \quad (19)$$

Fig. 8 illustrates the relationship between the beat dynamics of the linearized system and the corresponding phase variables, $\theta(t)$ and $\Delta(t)$. The coordinates $u_i(t)$, ($i = 1, 2$) represent exact analytical solution under the initial conditions obtained from (6) at $t = 0$. The integral G is calculated at the amplitude point¹, $\theta_0 = \pi/2 - 0.01$, chosen slightly below its maximal possible magnitude $\pi/2$. Since $\Delta = 0$ as $\theta = \theta_0$, then $G = -\cos \theta_0$ and therefore $\phi(t) = \varepsilon \Omega t$. Other parameters are taken as $\varepsilon = 0.01$, $\Omega = 1.0$, $K = 1.0$ and $\delta(0) = 0$. As follows from Fig. 8, the behavior of phase variables θ and Δ resembles smoothed time histories of the coordinate and velocity of a simple impact oscillator. As mentioned in Introduction, this fact was noticed first in [12], [14] based on the analysis of phase equations similar to (11) however obtained in a different way after complexification of the original coordinates. In particular, it was found that the ‘impact limit’ corresponds to the most intensive energy exchange between the oscillators when each of the oscillators periodically hosts the total energy of the system. It is seen now that, in the linearized case, such asymptotic follows directly from exact solutions, (18) and (19),

$$\begin{aligned} \theta(t) &\rightarrow \arcsin(\sin \phi) = \frac{\pi}{2} \tau \left(\frac{2}{\pi} \phi \right) \\ \Delta(t) &\rightarrow \arcsin \left(\frac{\cos \phi}{|\cos \phi|} \right) = \frac{\pi}{2} e \left(\frac{2\phi}{\pi} \right) \\ \phi &= \varepsilon \Omega t, \quad \theta_0 \rightarrow \pi/2 \end{aligned} \quad (20)$$

¹The notation θ_0 should not be confused with the initial value, which is $\theta(0) = 0$, according to the present form of the solution.

where $\tau(z)$ and $e(z)$ are triangular sine and rectangular cosine wave functions whose amplitude is unity and the period is normalized to four in order to provide the basic relationships of nonsmooth temporal transformations [21], $\tau'(z) = e(z)$ and $e^2(z) = 1$.

Now substituting (18) in (7), gives

$$\begin{aligned} E_1 &= \frac{1}{2}E_0(1 - \sin \theta_0 \sin \varepsilon\Omega t) \\ E_2 &= \frac{1}{2}E_0(1 + \sin \theta_0 \sin \varepsilon\Omega t) \end{aligned} \quad (21)$$

Taking into account (9) and (21), gives the corresponding energy partition index

$$P(t) = -\sin \theta_0 \sin \varepsilon\Omega t \quad (22)$$

Recall that the number $P = 0$ indicates equipartition, $E_1 = E_2$, whereas $P = 1$ or $P = -1$ correspond to the case when all the energy belongs to either first or second oscillator, respectively. As follows from (22), such states can be reached only in the limit case (20), when $\theta_0 = \pi/2$.

In case of small amplitudes $|\theta_0| \ll \pi/2$, corresponding to a moderate energy exchange, solutions (18) and (19) are approaching another simple limit of harmonic temporal shapes as illustrated by Fig. 9, where the amplitude is $\theta_0 = 0.5$. This also follows directly from the linearization of equation (16) near zero $\theta = 0$.

4.2 Nonlinear case

In this subsection, explicit analytical solution of the EP oscillator is obtained via transition to the action-angle variables, $\{\theta, \theta'\} \rightarrow \{I, \phi\}$, of the generating model, $\kappa = 0$. Re-scaling the time, $p = \varepsilon\Omega Gt$, brings the effective Hamiltonian of EP oscillator (17) to the form

$$H_p = \frac{H_\theta}{(\varepsilon\Omega G)^2} = \frac{1}{2}(\theta'^2 + \tan^2 \theta + \mu \cos 2\theta) \quad (23)$$

where $\theta' = d\theta/dp$ is interpreted as a linear momentum, $\mu = \kappa^2/(8G^2)$ is another parameter associated with the nonlinearity of Duffing oscillators κ defined by (12), and the quantity G given by (15) must be treated as a fixed number.

Based on the exact solution (18), the action-angle variables are introduced as follows [22], [21]

$$\begin{aligned} \theta &= \arcsin \left(\frac{\sqrt{2I + I^2}}{1 + I} \sin \phi \right) \\ \theta' &= \frac{(1 + I) \sqrt{2I + I^2} \cos \phi}{\sqrt{1 + (2I + I^2) \cos^2 \phi}} \end{aligned} \quad (24)$$

Now canonical transformation (24) brings Hamiltonian (23) and the corresponding differential equations of motion to the form

$$H_p = I + \frac{1}{2}I^2 + \frac{\mu}{2} \frac{1 + I(2 + I) \cos 2\phi}{(1 + I)^2} \quad (25)$$

and

$$\begin{aligned} \frac{dI}{dp} &= -\frac{\partial H_p}{\partial \phi} \equiv \mu \frac{I(2 + I)}{(1 + I)^2} \sin 2\phi \\ \frac{d\phi}{dp} &= \frac{\partial H_p}{\partial I} \equiv 1 + I - \frac{2\mu}{(1 + I)^3} \sin^2 \phi \end{aligned} \quad (26)$$

The essential advantage of new system (26) is that it becomes linear as $\mu = 0$ while the original oscillator (23) still remains strongly nonlinear. The idea of averaging can be also implemented as asymptotic integration of system (26) by means of the coordinate transformation $\{I, \phi\} \rightarrow \{J, \psi\}$:

$$\begin{aligned} I &= J - \mu \frac{J(2 + J)}{2(1 + J)^3} \cos 2\psi + O(\mu^2) \\ \phi &= \psi - \mu \frac{(J^2 + 2J - 2)}{4(1 + J)^4} \sin 2\psi + O(\mu^2) \end{aligned} \quad (27)$$

Transformation (27) is obtained from the condition eliminating the fast phase φ from the terms of order μ on the right-hand side in such a way that the new system takes the form

$$\begin{aligned} \frac{dJ}{dp} &= O(\mu^2) \\ \frac{d\psi}{dp} &= 1 + J - \frac{\mu}{(1 + J)^3} + O(\mu^2) \end{aligned} \quad (28)$$

System (28) is easily integrated as follows

$$\begin{aligned} J &= J_0 \\ \psi &= \left[1 + J - \frac{\mu}{(1 + J)^3} \right] p + \psi_0 \end{aligned} \quad (29)$$

where J_0 and ψ_0 are constants of integration.

Finally, substituting (29) in (27) and then (27) in (24), gives solution $\theta(p)$ whose effectiveness is illustrated by Figs. 10 and 11 at different nonlinearity and intensity of energy exchange levels, κ and P_0 , respectively. In particular, the transition from harmonic to sawtooth temporal shape of the phase θ is due to the increase of the amplitude of energy partition index, P_0 . The nonlinearity parameter κ has certain effect on the curvature of lines as seen from Fig. 11. Note that, although the above procedure of asymptotic integration assumes the parameter $\mu(\kappa)$ to be small as compared to unity, the solution appears to be

very effective also under quite significant magnitudes of μ provided that the corresponding trajectory holds its symmetry on the phase plane θ - θ' . However, the error of solution is growing as its trajectory becomes close to the separatrix of EP oscillator, which occurs under the condition $\kappa > 1$; see Section 5 for physical interpretation. Such situation appears to be quite common due to highly sensitive dynamics near separatrix loop.

Besides, expressions (27) and (29) point to the fact that, as the parameter μ increases, the monotonic growth of angle coordinate ϕ can be broken. This is confirmed also by the direct numerical integration of equations (26) at different magnitudes of the parameter μ as illustrated by Fig. 12. The initial angle is $\phi = \pi/2$ that associates with the extremum of the energy partition index P . The new action variable is fixed as $J = 1.0$, while the parameter μ is incrementally increased. As follows from the notations, this is eventually equivalent to incremental change of both the energy parameter κ and the amplitude of energy partition index, P_0 . Detailed calculations show that above approximately $\mu = 3.559$ ($\kappa = 1.4549$ and $P_0 = -0.927062$) the angle coordinate locks near its initial value $\phi = \pi/2$, as a result trajectories on the planes represented by Fig. 12 become closed.

5 MODE LOCALIZATION

The mode localization effect is shown schematically in Fig. 1. As mentioned in Section 3, the equilibrium points of oscillator (16) represent nonlinear normal modes of the original system. Although, in the case $\kappa \neq 0$, oscillator (16) is still solvable in quadratures, let us consider the following cubic approximation, by assuming that $|\theta| \ll \pi/2$,

$$\ddot{\theta} + (\varepsilon\Omega)^2 \left[\left(G^2 - \frac{\kappa^2}{4} \right) \theta + \frac{1}{6} (8G^2 + \kappa^2) \theta^3 \right] = 0 \quad (30)$$

As follows from (7), the equilibrium point $\theta = 0$ of oscillator (30) corresponds to the equal energy distribution, under which the original model (1) remains in one of its two symmetric nonlinear normal modes. So when the linear stiffness is positive, equation (30) has periodic solutions describing the energy exchange between oscillators (5) near in-phase or out-of-phase mode. However, the equal energy distribution, associated with the equilibrium $\theta = 0$, becomes unstable if the linear stiffness is negative, $G^2 - \kappa^2/4 < 0$. In this case two new stable equilibria surrounded by separatrix loops occur near the unstable equilibrium. This indicates the onset of nonlinear local modes of the original system (5) with a sustainable disbalance in the energy distribution despite of the perfect symmetry of system (1). In terms of the present notations, the condition of negative linear stiffness can be represented in the form [21]

$$f_2 \equiv -\frac{\kappa(2 - P_0^2)}{2\sqrt{1 - P_0^2}} < Q_0 < \frac{\kappa P_0^2}{2\sqrt{1 - P_0^2}} \equiv f_1 \quad (31)$$

where $P_0 = -\sin \theta_0$ and $Q_0 = -\cos \Delta_0$ the initial energy partition index as defined by (9).

Condition (31) constitutes a necessary condition of localization because it does not guarantee that the dynamics is trapped inside one of the separatrix loops. The corresponding sufficient condition is obtained from the energy integral of oscillator (30) in the form inequalities, first of which never holds for positive κ ,

$$\begin{aligned} Q_0 &> \frac{2 + \kappa P_0^2}{2\sqrt{1 - P_0^2}} \equiv g_1 \\ Q_0 &< -\frac{2 - \kappa P_0^2}{2\sqrt{1 - P_0^2}} \equiv g_2 \end{aligned} \quad (32)$$

Both estimates (31) and (32) are also valid locally, in the neighborhood of zero $\theta = 0$, for strongly nonlinear oscillator (17).

The above conditions (31) and (32) must be considered under the obvious constraint $|Q_0| \leq 1$. Fig. 13 illustrates a relatively low nonlinearity case, when localization is impossible. The solid lines represent the boundary functions, introduced in (31) and (32), whereas the couple of dashed lines indicates the rectangular area within which solutions of inequalities (31) and (32) the above mentioned constraint. When the strength of nonlinearity κ is increased, the line g_2 moves upward, whereas the line f_2 moves downward. When passing one through another at about $\kappa = 1$, two small areas of localization occur as shown in Fig. 14. Note that, in both localization areas, the initial phase angle Δ lays in the neighborhood of zero. Therefore, according to (6), the localized modes branch out of the out-of-phase modes as the nonlinearity becomes sufficiently strong.

6 THE BJJ FORMALISM

6.1 Classical resonance of coupled oscillators

The advantage of using the phase angle θ develops through the form of oscillator (16), which, in particular, admits clear qualitative analyses and allows for explicit analytical solution in terms of elementary functions when $\kappa = 0$. This fact is essentially employed in Section 4.2. In this section, however, the energy partition index P will be used instead of the phase angle θ in order to track the analogies with conventional approaches of macroscopic quantum dynamics as discussed in Section 6.2 below. Taking into account (9) and eliminating the angle θ from (6) and (11), gives the coordinate transformation and the resultant

differential equations in the form, respectively,

$$\begin{aligned}
u_1 &= \sqrt{\frac{1}{2}K(1+P)} \cos \delta \\
v_1 &= -\Omega \sqrt{\frac{1}{2}K(1+P)} \sin \delta \\
u_2 &= -\sqrt{\frac{1}{2}K(1-P)} \cos(\delta + \Delta) \\
v_2 &= \Omega \sqrt{\frac{1}{2}K(1-P)} \sin(\delta + \Delta)
\end{aligned} \tag{33}$$

and

$$\begin{aligned}
\dot{P} &= -\varepsilon\Omega \sqrt{1-P^2} \sin \Delta \equiv -\frac{\partial H_{eff}}{\partial \Delta} \\
\dot{\Delta} &= -\varepsilon\Omega \left(\kappa P - \frac{P \cos \Delta}{\sqrt{1-P^2}} \right) \equiv \frac{\partial H_{eff}}{\partial P}
\end{aligned} \tag{34}$$

where

$$\begin{aligned}
H_{eff} &= -\varepsilon\Omega \left(\frac{1}{2}\kappa P^2 + \cos \Delta \sqrt{1-P^2} \right) \\
&= \varepsilon\Omega \left(G - \frac{1}{2}\kappa \right)
\end{aligned} \tag{35}$$

and G is the result of substitution (9) in (15).

System (34) appears to have the form of BJJ describing the interaction of two Bose-Einstein condensates in macroscopic quantum dynamics [27] [25]. Further details of this analogy are discussed below in the present section. Equations (34) are solved independently on the fast phase δ , which is determined then by integration from

$$\dot{\delta} = \Omega + \frac{1}{2}\varepsilon\Omega \left[\kappa(1+P) + \cos \Delta \sqrt{\frac{1-P}{1+P}} \right] \tag{36}$$

Note that the effective Hamiltonian (35) can be obtained directly by substituting (33) in (3) and averaging the result with respect to the phase δ as follows

$$H_{eff} = -\frac{4}{K\Omega} \langle H \rangle_\delta + 2\Omega + \frac{1}{2}\varepsilon\Omega\kappa \tag{37}$$

Comparing the left-hand sides of equations (35) and (37) reveals the nature of integral (15), which is the constant mean value of the Hamiltonian, $\langle H \rangle_\delta = const.$ It was already mentioned that, from the mathematical standpoint, the Hamiltonian system (34) and (35) with its simplifications is similar to that usually appears in macroscopic quantum dynamics as Josephson junction equations; see Subsection 6.2 for references and details. It known that such

systems are exactly solvable in terms of elliptic functions [27], [25]. Eliminating the angle Δ in (35) by means of the first equation system (34), gives

$$\dot{P}^2 = (\varepsilon\Omega)^2 \left[1 - P^2 - \left(\frac{1}{2}\kappa P^2 - H_0 \right)^2 \right] \quad (38)$$

where $H_0 = -H_{eff}/(\varepsilon\Omega)|_{t=0}$.

Further manipulations leading to the elliptic functions are described in [25]. In particular, equation (38) gives the following quadrature

$$\frac{\varepsilon\Omega\kappa t}{2} = \int_{P(t)}^{P(0)} \frac{dz}{\sqrt{(a^2 + z^2)(c^2 - z^2)}} \quad (39)$$

where the parameters a and c are given by

$$\begin{aligned} a^2 c^2 &= \frac{4}{\kappa^2} (1 - H_0^2) \\ a^2 - c^2 &= \frac{4}{\kappa^2} (1 - \kappa H_0) \end{aligned}$$

Below, a series of diagrams (Figs. 15 and 16) provide qualitative descriptions of the dynamics in both $\Delta - P$ and $Q - P$ planes.

The evolution of topological structure of Hamiltonian (35) with gradually increasing nonlinearity levels is illustrated in Fig. 15. Similar diagrams were obtained in [25] for the case of two weakly coupled Bose-Einstein condensates. Classical nonlinear oscillatory chains were analyzed in somewhat different coordinates in [15], and when investigating the intensity of energy exchange between parts of periodic nonlinear Frenkel-Kontorova and Klein-Gordon lattices based on the concept of limiting phase trajectories [28].

As mentioned at the end of Section 2, the number of stationary points within the area, corresponding to rectangular (14), is increased by two when the nonlinearity parameter goes above the bifurcation level $\kappa = 1$. The new points, whose images are denoted by L in Fig. 15(c), correspond to the so-called *local modes* of the coupled Duffing oscillators branching out of the out-of-phase mode O ; see also Fig. 1. As follows from the diagrams Fig. 15 (c-d), near the points L , the energy partition index P preserves its signature, in other words, the energy is accumulated in mostly one of the two oscillators despite of the perfect symmetry of the mechanical model. If the initial state $(\Delta(0), P(0))$ lays outside but still close to the separatrix loop, which goes through the the image of out-of-phase mode O , the dynamics is not localized any more but combines the effects of two stable local (L) and one unstable out-of-phase (O) modes. Such a combination becomes impossible however as further increase of the nonlinearity level κ leads to the structural transition in the phase portrait such that the separatrix loop closes around the image of in-phase mode (I) rather than local modes (L). As a result, possible dynamics develop either near the in-phase mode or near one of the two local modes. Note that at high nonlinearity levels, $\kappa \gg 1$, the contour lines of effective Hamiltonian (35) resemble the phase portrait of classic

pendulum as follows, for instance, from Fig. 15 (d). Based on such similarity, it is possible to simplify the effective Hamiltonian (35) as follows

$$H_{eff} \longrightarrow H_J = -\varepsilon\Omega \left(\frac{1}{2}\kappa P^2 + \cos \Delta \right) \quad (40)$$

The effect of such simplification on the contour lines, however, would lead to disappearance of stationary points L corresponding to the local modes. Hamiltonian (40) gives the equation of pendulum whose angle is measured from the inverted (unstable) equilibrium

$$\ddot{\Delta} = (\varepsilon\Omega)^2 \kappa \sin \Delta \quad (41)$$

Note that the conventional phase difference used in the macroscopic quantum dynamics is $\Phi = \pi - \Delta$. The rigid pendulum analogy represents a typical reduction of SJJ equations describing the interaction of two weakly coupled superconductors, where Φ is a relative phase, and P is a fractional population imbalance [25]. However, the BJJ in a double-well trap still requires the complete form of equations.

Finally, using definitions (9) and (10), brings the diagrams of Fig. 15 to the form represented by Fig. 16. This gives a direct interpretation of the dynamics in terms of the energy partition and coherency indexes. In particular, the diagrams of Fig. 16 fully comply with the understanding of nonlinear normal modes as coherent motions of the system particles [30]. Namely, the normal modes correspond to the stationary points located on the vertical lines $Q = \pm 1$. In other words, when the energy partition index P is fixed, the oscillators coherently vibrate either in-phase ($Q = +1$) or out-of-phase ($Q = -1$), according to the definition of normal modes. On the configuration plane $u_1 u_2$, such type of motions is represented by pieces of lines passed by the system twice per one period. However, when the initial combination $P(0)$ and $Q(0)$ does not coincide with a stationary point then, during the vibrating process, both indexes slowly move along some trajectory on the plane PQ as shown in Fig. 16.

6.2 Macroscopic quantum dynamics

For comparison reason, let us reproduce few basic steps of the BJJ derivation in macroscopic quantum dynamics. Consider a two-level quantum system whose dynamics is described by the discrete version of nonlinear Schrödinger (Gross-Pitaevskii) equation [5] [23] ($\hbar=1$)

$$i \frac{d\psi_j}{dt} = \frac{\partial H}{\partial \psi_j^*} \quad (42)$$

where $\psi_j = \psi_j(t)$ ($j = 1, 2$) are complex amplitudes of the wave function ψ , and H is the system energy given by

$$H = \frac{V}{2}(\psi_1^* \psi_2 + \psi_1 \psi_2^*) + \frac{R}{2}(\psi_1^* \psi_1 - \psi_2 \psi_2^*) - \frac{c}{4}(\psi_1^* \psi_1 - \psi_2 \psi_2^*)^2 \quad (43)$$

Here V is the strength of coupling between two modes, while c is the strength of interaction between atoms, R characterizes the energy difference between two wells (bias). For the purpose of present work, it can be assumed that $R = 0$ [4]; as a result, equation (42) gives

$$\begin{aligned} i \frac{d\psi_1}{dt} &= \frac{V}{2}\psi_2 - \frac{c}{2}(\psi_1^*\psi_1 - \psi_2\psi_2^*)\psi_1 \\ i \frac{d\psi_2}{dt} &= \frac{V}{2}\psi_1 + \frac{c}{2}(\psi_1^*\psi_1 - \psi_2\psi_2^*)\psi_2 \end{aligned} \quad (44)$$

In the literature, this model can be found in different physical contents and somewhat different notations [18], [27], [25], [31], [10]. In general terms, it describes the tunneling effect in two coupled Bose-Einstein condensates.

The following complexification of transformation (33) is applied now,

$$\begin{aligned} \psi_1 &= \sqrt{\frac{1}{2}K(1+P)} \exp(\delta i) \\ \psi_2 &= -\sqrt{\frac{1}{2}K(1-P)} \exp[(\delta + \Delta)i] \end{aligned} \quad (45)$$

where, the normalization condition for probability, $|\psi_1|^2 + |\psi_2|^2 = 1$, takes the form $K = 1$, and physical interpretation of the energy partition index P may depend upon the problem formulation.

Substituting (45) in (44), gives equation for the fast phase δ ,

$$\dot{\delta} = \frac{c}{2}P + \frac{V}{2}\sqrt{\frac{1-P}{1+P}} \cos \Delta \quad (46)$$

and the following classical Hamiltonian system for the canonically conjugate variables P - Δ ,

$$\begin{aligned} \dot{P} &= -V\sqrt{1-P^2} \sin \Delta \equiv -\frac{\partial H_{eff}}{\partial \Delta} \\ \dot{\Delta} &= -cP + V\frac{P \cos \Delta}{\sqrt{1-P^2}} \equiv \frac{\partial H_{eff}}{\partial P} \end{aligned} \quad (47)$$

where H_{eff} is so-called effective Josephson Hamiltonian

$$H_{eff} = -\left(\frac{1}{2}cP^2 + V \cos \Delta \sqrt{1-P^2}\right) \quad (48)$$

More often, however, the term Josephson Hamiltonian is used for a simplified version of (48), associated with the classical rigid pendulum as discussed at the end of Section 6.1. Note that substitution of (45) directly into the original Hamiltonian gives

$$H_{eff} = 2H \quad (49)$$

Although the numerical factor in this relationship can be eliminated by rescaling the time variable, nevertheless the presence of such factor moves transformation (45) out of the class of canonical transformations. This problem can be fixed [11], however, at cost of losing the traditional form Josephson's system.

Despite the fact that the original system is quantum by formulation, the effective model (47) through (48) is usually qualified as a classical Hamiltonian system since the variables P - Δ can be simultaneously determined provided that it is true for their initial values. System (47) is equivalent to (34) under the conditions $\varepsilon\Omega = V$ and $\kappa = c/V$. Substituting $P(t) = -\sin\theta(t)$ in (47) and (48), and eliminating the phase Δ , gives the effective conservative oscillator, similar to that was introduced for the case of coupled Duffing oscillators,

$$\ddot{\theta} + \left(H_{eff} + \frac{c}{2}\right)^2 \frac{\tan\theta}{\cos^2\theta} - \frac{1}{8}c^2 \sin 2\theta = 0 \quad (50)$$

where the number H_{eff} must be calculated by fixing a trajectory on the plane $P - \Delta$ or $\theta - \Delta$ before the oscillator is (50) is solved.

Introducing the new time scale $p = (H_{eff} + c/2)t$ and the parameter $\mu = (1/2)(1 + 2H_{eff}/c)^{-2}$ enables one of using the solution in terms of elementary functions obtained in Section 4.2 for the case of coupled Duffing oscillators.

6.3 Further analogies

In terms of the macroscopic phase difference $\Phi = \phi_r - \phi_l$, corresponding to the right (r) and left (l) wells, and the atom number difference $k = (N_l - N_r)/2$, Josephson type equations for the case symmetric double-well potential are obtained from Gross-Pitaevskii theory [27], [25]

$$\begin{aligned} \dot{k} &= -E_J \sqrt{1 - 4k^2/N^2} \sin \Phi \\ \dot{\Phi} &= E_C k + \frac{4k/N^2}{\sqrt{1 - 4k^2/N^2}} E_J \cos \Phi \end{aligned} \quad (51)$$

where $N = N_l + N_r$ is the total number of atoms; E_J and E_C and are called tunneling and charging energies, respectively, measured in units \hbar . The charging energy arises from interatomic interactions, the tunneling energy determines the maximum current $I_J = E_J$.

Introducing notations,

$$\begin{aligned} P &= \frac{2k}{N} = \frac{N_l - N_r}{N_l + N_r} \\ \Delta &= \pi - \Phi \end{aligned} \quad (52)$$

brings system (51) exactly to the Hamiltonian form (34)-(35), after the following parameter substitutions

$$\begin{aligned} \varepsilon\Omega &= \frac{2E_J}{N} \\ \kappa &= \frac{N^2 E_C}{4 E_J} \end{aligned} \quad (53)$$

Moreover, re-scaling the time variable as $\varepsilon\Omega t = \bar{t}$ in (34) and $2(E_J/N)t = \bar{t}$ in (51), brings both systems to the same single parameter form [27], [25]

$$\begin{aligned}\frac{dP}{d\bar{t}} &= -\sqrt{1-P^2} \sin \Phi \\ \frac{d\Phi}{d\bar{t}} &= \kappa P + \frac{P}{\sqrt{1-P^2}} \cos \Phi\end{aligned}\quad (54)$$

where the strength of nonlinearity of Duffing system (12) κ becomes equivalent to the parameter Λ [27], the energy partition index between the Duffing oscillators, P , is equivalent to the fractional relative population, and the phase shift between the Duffing oscillators, Φ , is the quantum phase difference between the right and left components.

In order to use the results sections 3, 4.1, and 4.2, the fractional relative population P must be expressed through the phase angle θ . This leads to the integral

$$H_\theta \equiv \frac{1}{2}\dot{\theta}^2 + \frac{1}{2}\left(H_{eff} + \frac{NE_C}{4}\right)^2 \tan^2 \theta + \left(\frac{NE_C}{8}\right)^2 \cos 2\theta \quad (55)$$

where H_{eff} is the effective Hamiltonian of system (51) calculated on a fixed trajectory.

Introducing the new time variable p and the action-angle variables (24) brings oscillator to its Hamiltonian form (26), where

$$\begin{aligned}p &= \left(H_{eff} + \frac{NE_C}{4}\right)t \\ \mu &= \frac{1}{2}\left(1 + \frac{4H_{eff}}{NE_C}\right)^{-2}\end{aligned}\quad (56)$$

Therefore, analytical solution (24) through (29) obtained in Section 4.2 for the angle θ , gives

$$P = \frac{N_l - N_r}{N_l + N_r} = -\sin \theta = -\frac{\sqrt{2I + I^2}}{1 + I} \sin \phi \quad (57)$$

where the action-angle variables, I and ϕ , are given by (27) and (29).

6.4 Second quantization

As discussed at the end of Section 6.1, system (51) becomes equivalent to the classical pendulum under the conditions $|P| \ll 1$ and $\kappa \gg 1$ whose physical meaning is revealed by (53). As result, Hamiltonian of system (51) is reduced to that of the classical pendulum

$$\begin{aligned}H_J &= \frac{E_C}{2}k^2 - E_J \cos \Phi \\ \dot{k} &= -\frac{\partial H_J}{\partial \Phi} = -E_J \sin \Phi \\ \dot{\Phi} &= \frac{\partial H_J}{\partial k} = E_C k\end{aligned}\quad (58)$$

Except some technical advantages, such simplification does not seem to be crucial from the standpoint of classical dynamics since both systems (51) and (58) are integrable. However, in contrast to (51), the Hamiltonian of system (58) has the quadratic form with respect to the ‘linear momentum’ k , which is important for the idea of second quantization [24]

$$\hat{H}_J = -\frac{E_C}{2} \frac{\partial^2}{\partial \Phi^2} - E_J \cos \Phi \quad (59)$$

Further discussion and references on the transition from (58) to (59) can be found in [9]. Note that the effective Hamiltonian of energy partition oscillator (55) is quadratic with respect to the ‘linear momentum’ θ so that no further simplification would be required from the standpoint of second quantization.

7 CONCLUDING REMARKS

This work points to interdisciplinary links between the resonance phenomena in classical nonlinear dynamics and tunneling effects considered in the macroscopic quantum dynamics. It is shown that the classical dynamics of 1:1 resonance interaction between two identical linearly coupled Duffing oscillators is equivalent to the symmetric (non-biased) case of ‘macroscopic’ quantum dynamics of two weakly coupled Bose-Einstein condensates. The analogy develops through the BJJ equations, however, reduced to a single conservative EP oscillator imposing no additional assumptions. The derived oscillator is solvable in quadratures, furthermore it admits asymptotic solution in terms of elementary functions after transition to the action-angle variables. The energy partition and coherency indexes are introduced to provide a complete characterization of the system dynamic states through the state variables of the EP oscillator. In particular, nonlinear normal and local mode dynamics of the original system associate with equilibrium points of the oscillator. Additional equilibrium points - the local modes - may occur on high energy level as a result of the symmetry breaking bifurcation. Further, it is shown that vibrations near nonlinear local modes of the coupled Duffing’s oscillators are equivalent to the macroscopic quantum self-trapping (MQST) effect. As discussed earlier [25], there are two types of MQST, such as running-phase MQST and π -phase MQST. While BJJ captures both types of MQST, the SJJ rigid pendulum approximation ignores the π -phase MQST. Finally, it is noticed that, since the Hamiltonian of EP oscillator is always quadratic with respect its linear momentum, the idea of second quantization can be explored in terms of BJJ without usual transition to the pendulum approximation. The quantum version of oscillator (55) allows for asymptotic limits with square well and sine-wave potentials, corresponding to the classic vibro-impact and harmonic oscillators, respectively.

APPENDIX

As mentioned in the text, substituting (6) in (5) and then solving the set of equations with respect to the derivatives, gives

$$\begin{aligned}
\dot{K} &= \varepsilon K \Omega \cos \theta \sin(2\delta + \Delta) + \frac{2\varepsilon\sqrt{K}}{\Omega} \\
&\quad \times \left[f_1 \cos\left(\frac{\theta}{2} + \frac{\pi}{4}\right) \sin \delta - f_2 \cos\left(\frac{\theta}{2} - \frac{\pi}{4}\right) \sin(\delta + \Delta) \right] \\
\dot{\theta} &= \varepsilon \Omega [\sin \Delta - \sin \theta \sin(2\delta + \Delta)] - \frac{2\varepsilon}{\sqrt{K}\Omega} \\
&\quad \times \left[f_1 \cos\left(\frac{\theta}{2} - \frac{\pi}{4}\right) \sin \delta + f_2 \cos\left(\frac{\theta}{2} + \frac{\pi}{4}\right) \sin(\delta + \Delta) \right] \\
\dot{\Delta} &= -\frac{2\varepsilon}{\sqrt{K}\Omega} \left\{ \Omega^2 \sqrt{K} \cos \delta \cos(\delta + \Delta) \tan \theta \right. \\
&\quad \left. + \sec \theta \left[f_1 \cos\left(\frac{\theta}{2} - \frac{\pi}{4}\right) \cos \delta + f_2 \cos\left(\frac{\theta}{2} + \frac{\pi}{4}\right) \cos(\delta + \Delta) \right] \right\} \\
\dot{\delta} &= \Omega \left[1 + \varepsilon \cos \delta \cos(\delta + \Delta) \tan\left(\frac{\theta}{2} + \frac{\pi}{4}\right) \right] \\
&\quad + \frac{\varepsilon}{\sqrt{K}\Omega} f_1 \cos \delta \sec\left(\frac{\theta}{2} + \frac{\pi}{4}\right)
\end{aligned} \tag{A1}$$

where $f_i = U'(u_i)$ and the coordinates u_i ($i = 1, 2$) are given by (6).

System (60) is still an exact equivalent to system (5) and represents a standard dynamic system with a single fast phase, δ . Applying the standard averaging procedure over the fast phase δ on the right-hand side of system (60), gives equations (11).

References

- [1] A. Barone and G. Paternò. *Physics and applications of the Josephson effect*. UMI books on demand. Wiley, 1982.
- [2] Franco Dalfovo, Stefano Giorgini, Lev P. Pitaevskii, and Sandro Stringari. Theory of bose-einstein condensation in trapped gases. *Rev. Mod. Phys.*, 71:463–512, Apr 1999.
- [3] M. F. Dimentberg and A. S. Bratus. Bounded parametric control of random vibrations. *R. Soc. Lond. Proc. Ser. A Math. Phys. Eng. Sci.*, 456(2002):2351–2363, 2000.
- [4] S. Giovanazzi, J. Esteve, and M. K. Oberthaler. Effective parameters for weakly coupled bose-einstein condensates. *New Journal of Physics*, 10(4):045009 (8pp), 2008.

- [5] E. P. Gross. Structure of a quantized vortex in boson systems. *Nuovo Cimento*, 20:454–477, 1961.
- [6] D. D. Holm and P. Lynch. Stepwise precession of the resonant swinging spring. *SIAM J. Applied Dynamical Systems*, 1(1):44–64, 2002.
- [7] H. Kauderer. *Nichtlineare Mechanik*. Springer-Verlag, Berlin, 1958.
- [8] A.M. Kosevich and A.S. Kovalev. *Introduction to Nonlinear Physical Mechanics (in Russian)*. Naukova Dumka, Kiev, 1989.
- [9] G. J. Krahn and D. H. J. O’Dell. Classical versus quantum dynamics of the atomic josephson junction. *Journal of Physics B: Atomic, Molecular and Optical Physics*, 42(20):205501, 2009.
- [10] Jie Liu, Libin Fu, Bi-Yiao Ou, Shi-Gang Chen, Dae-Il Choi, Biao Wu, and Qian Niu. Theory of nonlinear landau-zener tunneling. *Phys. Rev. A*, 66:023404, Aug 2002.
- [11] Jie Liu, Biao Wu, and Qian Niu. Nonlinear evolution of quantum states in the adiabatic regime. *Phys. Rev. Lett.*, 90:170404, May 2003.
- [12] L.I. Manevich. New approach to beating phenomenon in coupled nonlinear oscillatory chains. *Archive of Applied Mechanics*, 77:301–312, 2007.
- [13] L. I. Manevitch. Manevitch, new approach to beating phenomenon in coupled nonlinear oscillatory chains. *Proc. 8th Conference on Dynamical Systems - Theory and Applications, Lodz, 2005*, page 289, 2005.
- [14] L. I. Manevitch and A.I. Musienko. Limiting phase trajectory and beating phenomena in systems of coupled nonlinear oscillators. *2nd International Conference on Nonlinear Normal Modes and Localization in Vibrating Systems, Samos, Greece, June 19-23*, pages 25–26, 2006.
- [15] L. I. Manevitch and V. V. Smirnov. Limiting phase trajectories and the origin of energy localization in nonlinear oscillatory chains. *Phys. Rev. E*, 82:036602, Sep 2010.
- [16] L.I. Manevitch, A.S. Kovaleva, and D.S. Shepelev. Non-smooth approximations of the limiting phase trajectories for the duffing oscillator near 1:1 resonance. *Physica D: Nonlinear Phenomena*, 240(1):1 – 12, 2011.
- [17] L.I. Manevitch and V.V. Smirnov. Resonant energy exchange in nonlinear oscillatory chains and limiting phase trajectories: from small to large systems. *arXiv*, 0903.5455v1, 2009.
- [18] G. J. Milburn, J. Corney, E. M. Wright, and D. F. Walls. Quantum dynamics of an atomic bose-einstein condensate in a double-well potential. *Phys. Rev. A*, 55:4318–4324, Jun 1997.

- [19] S. V. Nesterov. Examples of nonlinear Klein-Gordon equations, solvable in terms of elementary functions. *Proceedings of Moscow Institute of Power Engineering*, 357:68–70, 1978.
- [20] V. N. Pilipchuk. Analytical study of vibrating systems with strong nonlinearities by employing saw-tooth time transformations. *J. Sound Vibration*, 192(1):43–64, 1996.
- [21] V. N. Pilipchuk. *Nonlinear Dynamics: Between Linear and Impact Limits (Lecture Notes in Applied and Computational Mechanics)*. Springer, 2010.
- [22] V.N. Pilipchuk. Transitions from strongly to weakly-nonlinear dynamics in a class of exactly solvable oscillators and nonlinear beat phenomena. *Nonlinear Dynamics*, 52(4):263–276, 2008.
- [23] L. P. Pitaevskii. Vortex lines in an imperfect bose gas. *Soviet Physics JETP*, 13:451454, 1961.
- [24] L.P. Pitaevskii and S. Stringari. *Bose-Einstein condensation*. International series of monographs on physics. Clarendon Press, 2003.
- [25] S. Raghavan, A. Smerzi, S. Fantoni, and S. R. Shenoy. Coherent oscillations between two weakly coupled bose-einstein condensates: Josephson effects, π oscillations, and macroscopic quantum self-trapping. *Phys. Rev. A*, 59:620–633, Jan 1999.
- [26] A. C. Scott, P. S. Lomdahl, and J. C. Eilbeck. Between the local-mode and normal-mode limits. *Chemical Physics Letters*, 113(1):29–36, 1985.
- [27] A. Smerzi, S. Fantoni, S. Giovanazzi, and S. R. Shenoy. Quantum coherent atomic tunneling between two trapped bose-einstein condensates. *Phys. Rev. Lett.*, 79:4950–4953, Dec 1997.
- [28] V.V. Smirnov and L. I. Manevitch. Limiting phase trajectories and dynamic transitions in nonlinear periodic systems. *Acoustical Physics*, 57(2):271–276, 2011.
- [29] Y. Starosvetsky and L. I. Manevitch. Nonstationary regimes in a duffing oscillator subject to biharmonic forcing near a primary resonance. *Phys. Rev. E*, 83:046211, Apr 2011.
- [30] A. F. Vakakis, L. I. Manevitch, Yu. V. Mikhlin, V. N. Pilipchuk, and A. A. Zevin. *Normal modes and localization in nonlinear systems*. John Wiley & Sons Inc., New York, 1996. A Wiley-Interscience Publication.
- [31] Biao Wu and Qian Niu. Nonlinear landau-zener tunneling. *Phys. Rev. A*, 61:023402, Jan 2000.

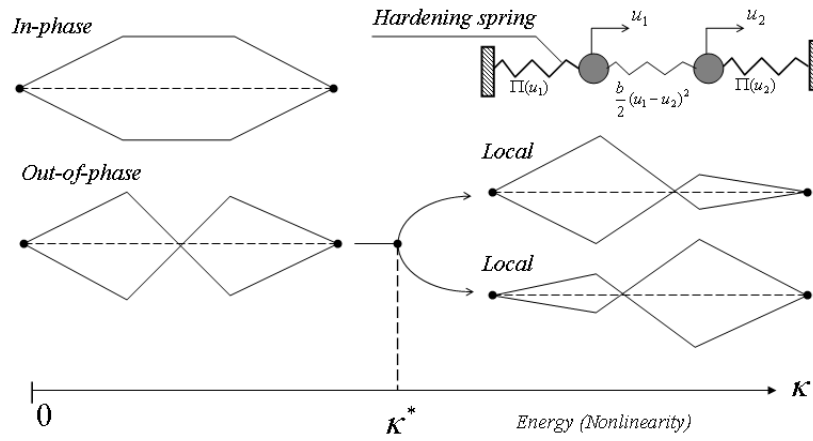


FIG.1. Nonlinear normal and local modes of the coupled Duffing oscillators with symmetry breaking bifurcation generating two stable local modes from the out-of-phase mode.

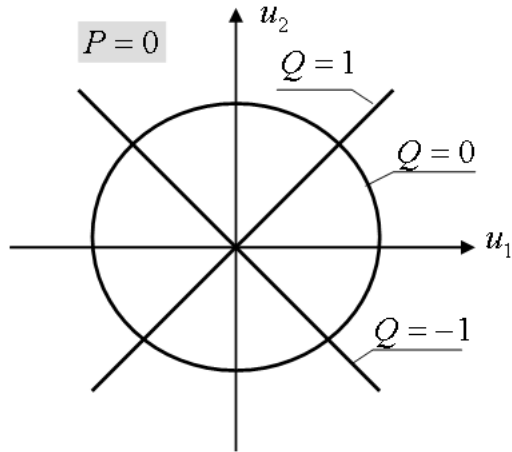


FIG.2. Geometrical interpretation of the coherency index on configuration plane in case of the energy equipartition, $P = 0$.

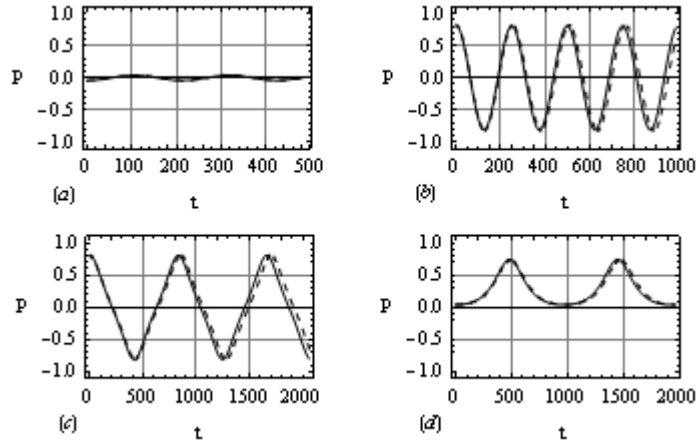


FIG.3. Time histories of the energy partition index on the supercritical nonlinearity (energy) level $\kappa = 1.2$ at different initial configurations of the model; see Fig. 4 for the corresponding trajectories on configuration plane.

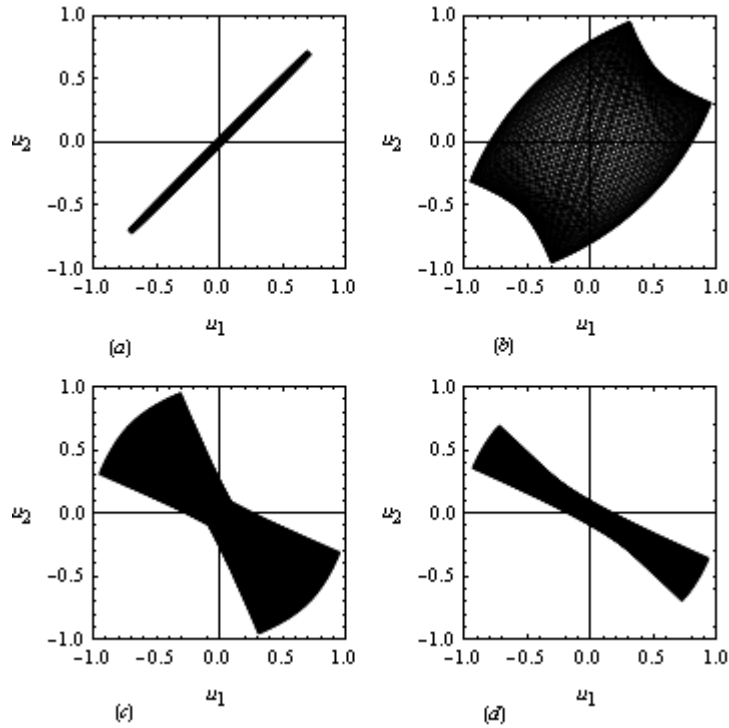


FIG.4. Configuration plane trajectories on the supercritical energy level, $\kappa = 1.2$, at different initial configurations of the model: (a) and (b) - the dynamics in small and large neighborhoods of the in-phase mode, respectively, (c) - the global dynamics around the unstable out-phase and both stable local modes, and (d) - the neighborhood

of one local mode; the corresponding energy partition index is shown in Fig. 3 (a) through (d), respectively, see also Fig. 5.

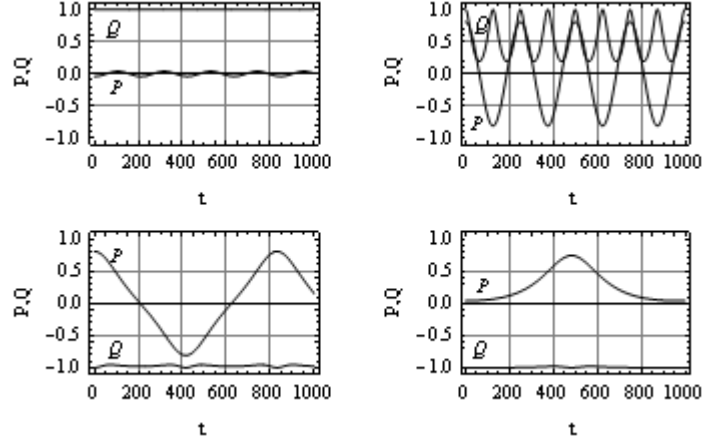


FIG.5. Energy partition and coherency indexes on the supercritical energy level, $\kappa = 1.2$, at different initial configurations of the model; see Fig. 4 for the corresponding trajectories on configuration plane.

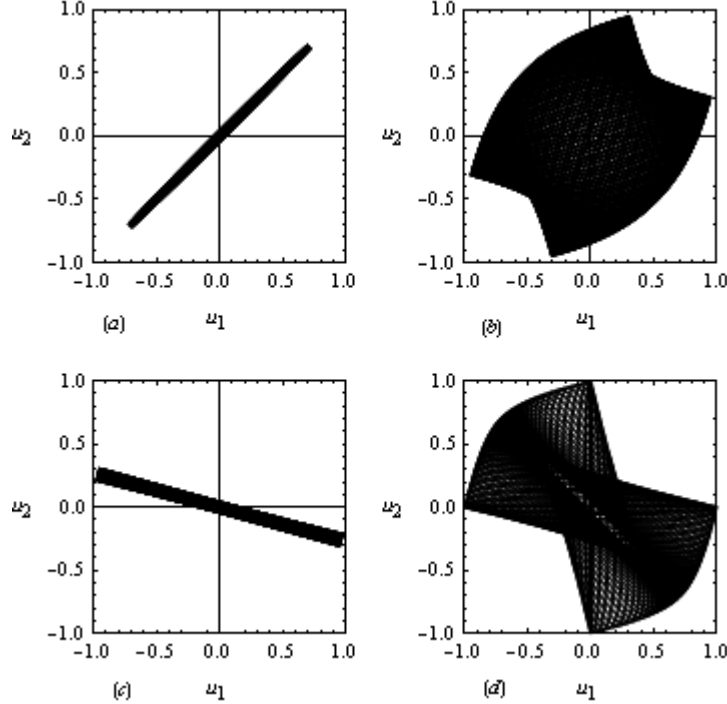


FIG.6. Configuration plane trajectories on the supercritical energy level, $\kappa = 2.0$: (a) and (b) - the dynamics in small and large neighborhoods of the in-phase mode,

respectively, (c) - the neighborhood of local mode, and (d) - the drift over unstable out-of-phase mode and two stable local modes; see Fig. 7 for the energy partition and coherency indexes.

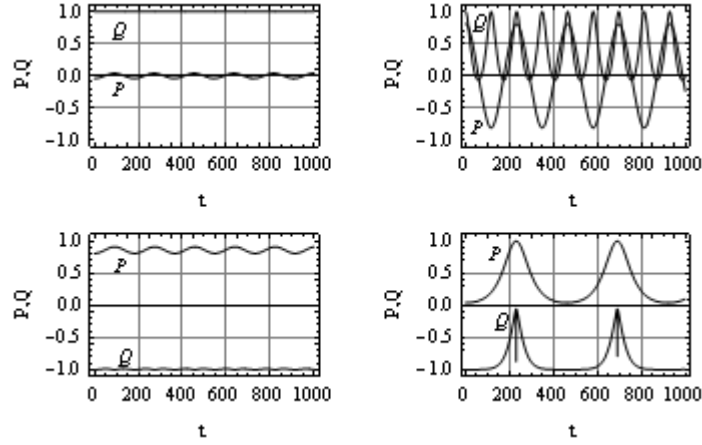


FIG.7. Energy partition and coherency indexes on the supercritical energy level, $\kappa = 2.0$, corresponding the dynamics illustrated by Fig. 6.

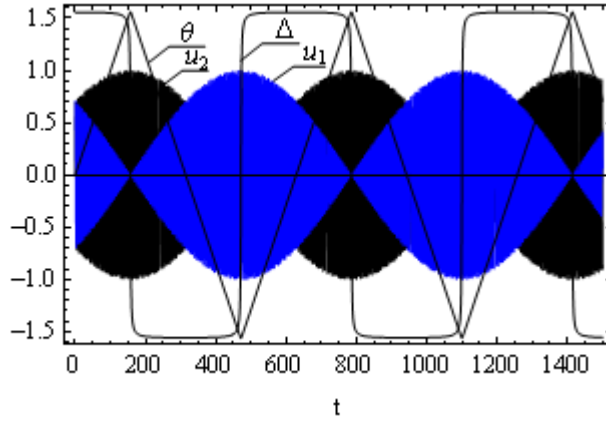


FIG.8. Exact solutions for the beat dynamics of two identical linearly coupled harmonic oscillators and associated phase variables of the EP oscillator; highly intensive energy exchange.

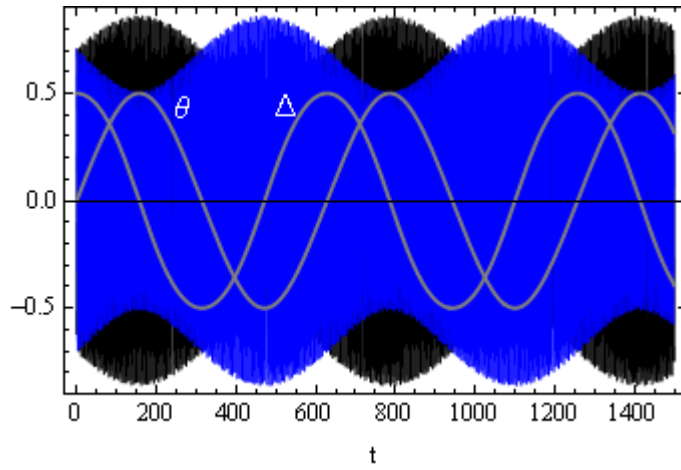


FIG.9. Same as Fig. 8; moderate energy exchange.

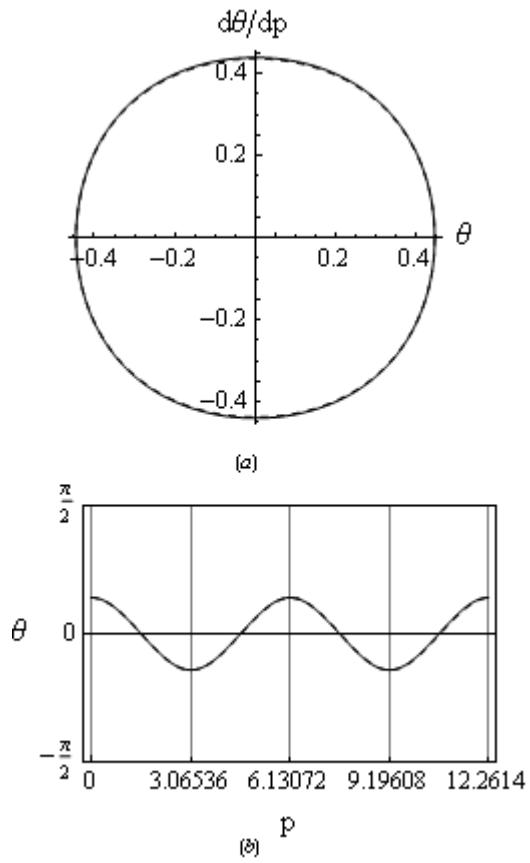


FIG.10. Analytical and numerical solutions represented by solid and dashed lines,

respectively, for $\kappa = 0.591728$ and $P_0 = -0.430443$; (a) phase trajectory, and (b) time history; $p = \varepsilon\Omega Gt$.

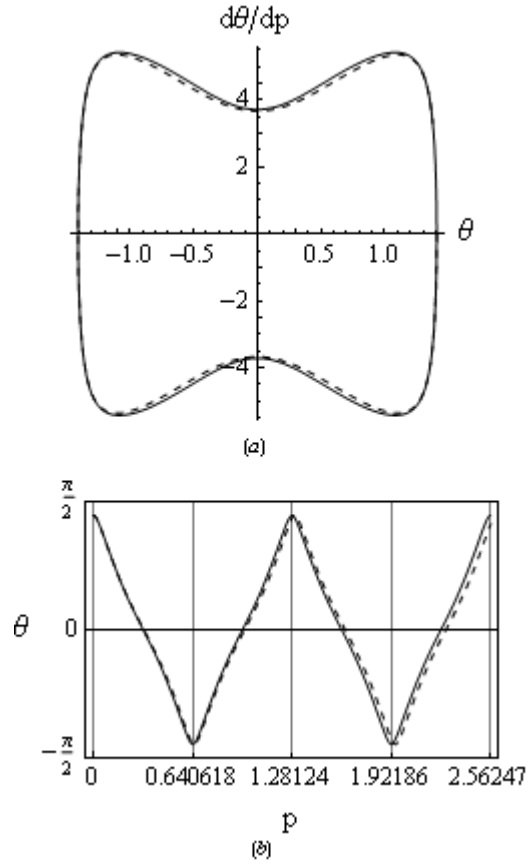


FIG.11. Analytical and numerical solutions represented by solid and dashed lines, respectively, for $\kappa = 1.41012$ and $P_0 = -0.986701$; (a) phase trajectory, and (b) time history; $p = \varepsilon\Omega Gt$.

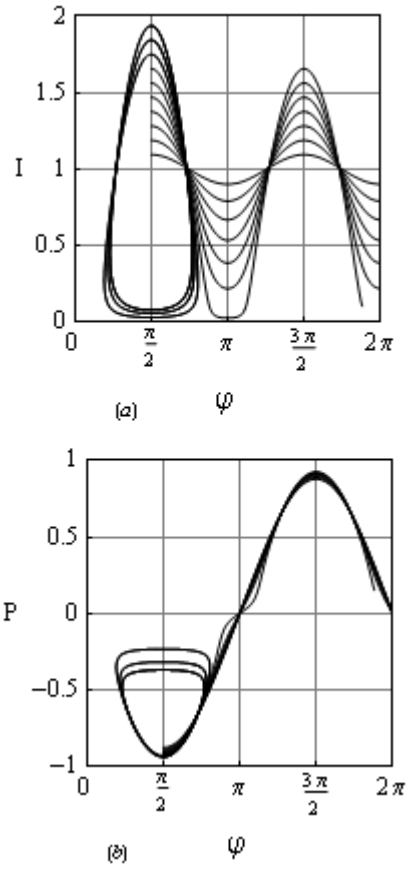


FIG.12. Angle trapping of the action-angle variables at high action levels (a), and its interpretation through the energy partition index (b); $J = 1.0$; $\mu = 0.5, 1.0, \dots, 5.0$.

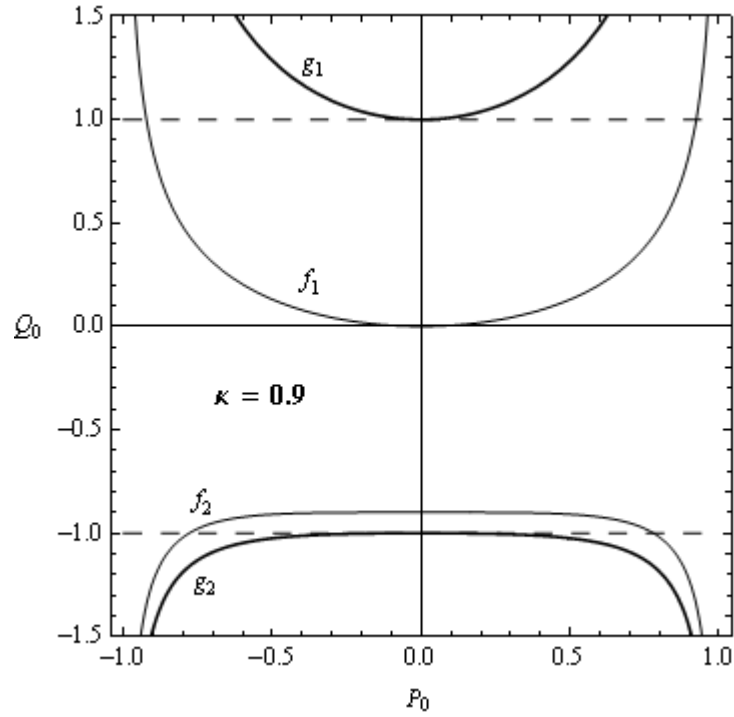


FIG.13. The plane of initial coherence versus energy partition showing no localization area at relatively low nonlinearity κ ; dashed horizontal lines bound the allowed region $|Q_0| \leq 1$.

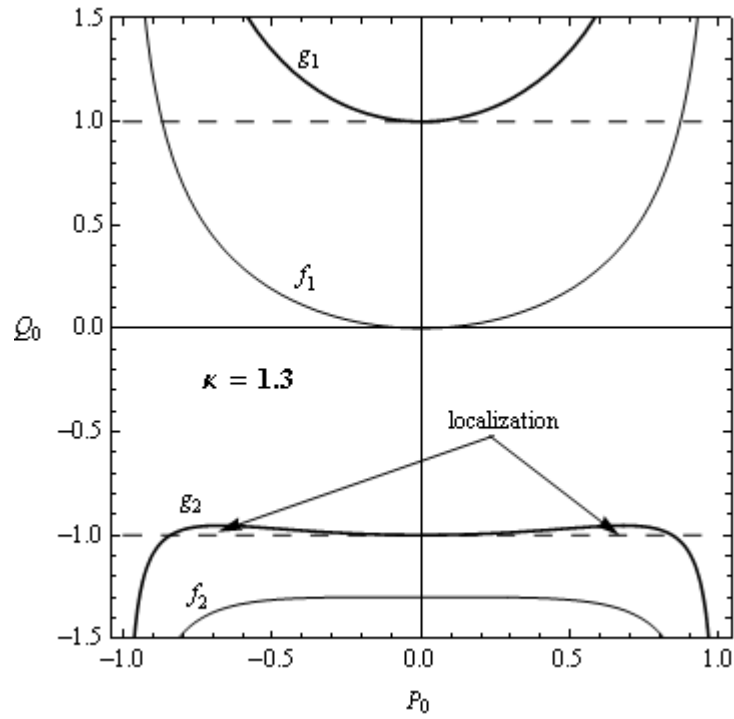


FIG.14. The plane of initial coherence versus energy partition showing two localization areas on higher nonlinearity level κ .

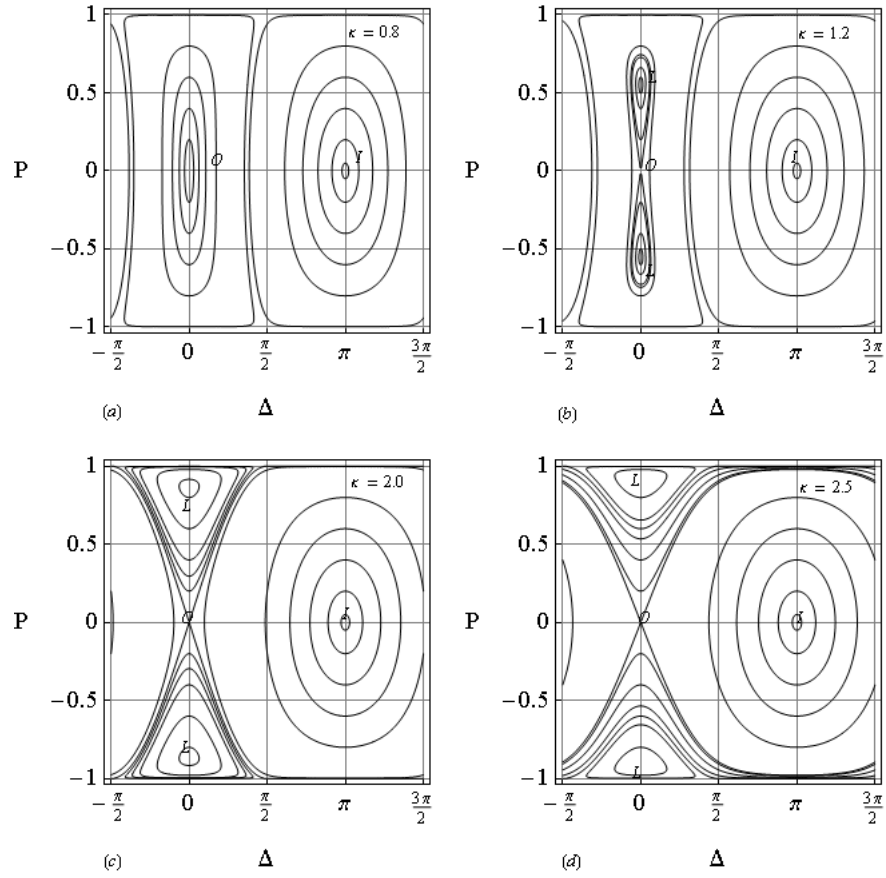


FIG.15. Contour lines of the effective Hamiltonian of the energy exchange equations between Duffing oscillators at different nonlinearity levels: (a) quasi linear case, (b) post-bifurcation case $\kappa = 1.2$ with center-saddle bifurcation near the out-of-phase mode, (c) strongly nonlinear multiple (>2) modes effect, and (d) strongly nonlinear effect of separatrix topological transition.

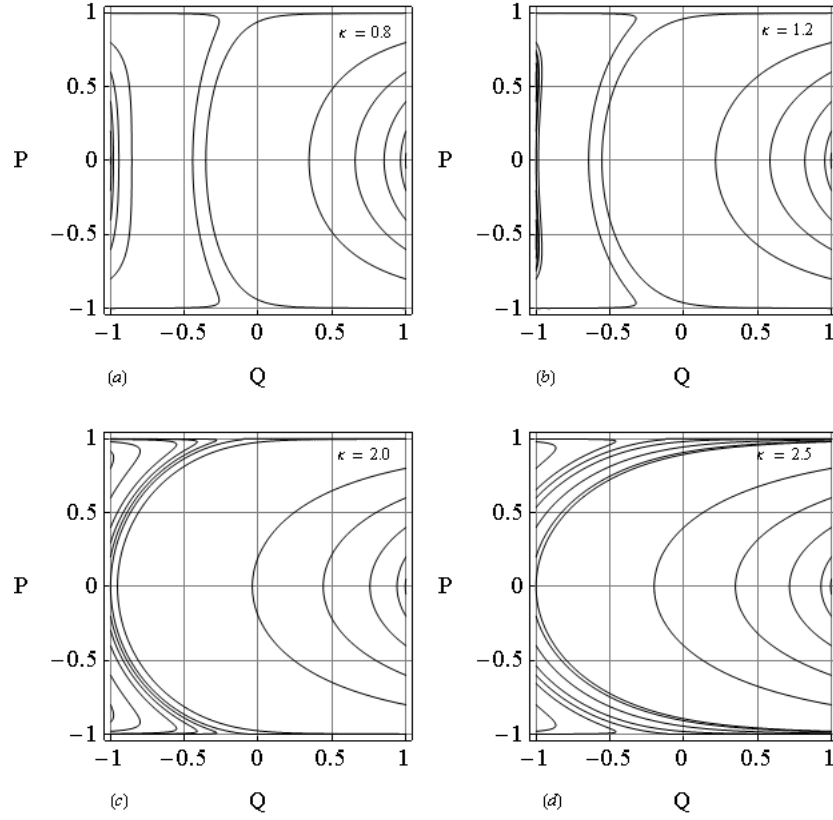


FIG.16. Energy partition versus coherency index diagrams at different nonlinearity levels: (a) quasi linear case, (b) post-bifurcation case $\kappa = 1.2$ with center-saddle bifurcation near the out-of-phase mode, (c) strongly nonlinear multiple (>2) modes effect, and (d) strongly nonlinear effect of separatrix topological transition.